Review — Magnetism, magnetic materials, and interdisciplinary research

Tuning the electrons at the $LaAlO_3/SrTiO_3$ interface: From growth to beyond growth*

Xie Yan-Wu(谢燕武)[a)b)†] and Hwang Harold Y[a)b)]

[a)] *Geballe Laboratory for Advanced Materials, Department of Applied Physics, Stanford University, Stanford, California* 94305, *USA*
[b)] *Stanford Institute for Materials and Energy Sciences, SLAC National Accelerator Laboratory, Menlo Park, California* 94025, *USA*

(Received 14 September 2013)

Recently, the quasi-two-dimensional electron gas (q2DEG) confined at the interface between $LaAlO_3$ and $SrTiO_3$ has attracted significant attention. In this paper, we briefly review experimental methods that have been used to tune the carrier density and mobility of this q2DEG. These methods can be classified into two categories: growth-related tuning (i.e. substrate, growth temperature, oxygen pressure, post-annealing, $LaAlO_3$ thickness, stoichiometry, and capping layers) and post-growth tuning (i.e. electrostatic field gating, conductive atomic force microscopy and surface adsorbates). Taken together, these methods enable the broad tuning of the electronic properties of this interface.

Keywords: $LaAlO_3/SrTiO_3$, strontium titanate, oxides, two-dimensional electron gas, interface

PACS: 73.20.–r, 73.40.–c, 75.70.cn **DOI:** 10.1088/1674-1056/22/12/127301

1. Introduction

In 2004 it was discovered[1] that the (001) interface between two wide-band insulators, $LaAlO_3$ (LAO, E_{gap} = 5.6 eV) and $SrTiO_3$ (STO, E_{gap} = 3.2 eV), can be highly conductive. It was suggested that this originates from the polar nature of LAO and the accurate control of the interface on an atomic scale.[2–4] As shown in Fig. 1(a), both LAO and STO have the same perovskite structure. From the ionic viewpoint in Fig. 1(b), STO is stacked alternatively with charge-neutral atomic layers of $(Sr^{2+}O^{2-})^0$ and $(Ti^{4+}O_2^{4-})^0$; in contrast, LAO is stacked with positively and negatively charged atomic layers of $(La^{3+}O^{2-})^{1+}$ and $(Al^{3+}O_2^{4-})^{1-}$. To match the perovskite structure, two kinds of interfaces, $(Sr^{2+}O^{2-})^0/(Al^{3+}O_2^{4-})^{1-}$ and $(Ti^{4+}O_2^{4-})^0/(La^{3+}O^{2-})^{1+}$, can be formed. It turns out that only the interface between $(Ti^{4+}O_2^{4-})^0$ and $(La^{3+}O^{2-})^{1+}$ is conducting for a wide range of growth parameters.[1,2] Experimentally, this interface is constructed by epitaxially growing a few unit cells (uc's) of LAO film on a TiO_2-terminated single-crystalline STO substrate. In a simplified electronic reconstruction picture,[2] such as the one sketched in Fig. 1(c), electrons move from the LAO surface to the interface to reconcile the divergent built-in potential produced by the alternatively stacked charged atomic layers in the LAO film forming the highly mobile electron gas. This simple picture is based on the assumption that the surface maintains a bulk-like stoichiometry.

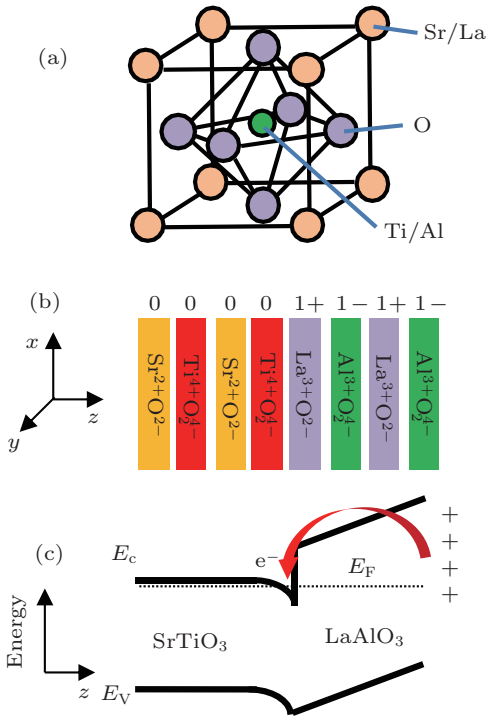


Fig. 1. Schematic crystal and band structure of LAO/STO. (a) The perovskite structure of STO and LAO. (b) From an ionic viewpoint, the atomic layers in STO are charge-neutral while those in LAO are stacked alternatively with positive and negative layers in the (001) direction. (c) Schematic energy band structure of LAO/STO. Electrons move from surface to interface to reconcile the built-in potential in the LAO film (for an unreconstructed surface).

A number of interesting properties, including high-mobility electrons,[1] two-dimensional (2D) superconductivity,[5,6] ferromagnetism,[7–9] and even the coexistence of superconductivity and ferromagnetism,[10–12] have been demon-

*Project supported by the Department of Energy, Office of Basic Energy Sciences (Grant No. DE-AC02-76SF00515). Xie Yan-Wu was also partially sponsored from the AFOSR-MURI on "Quantum Preservation, Simulation & Transfer in Oxide Nanostructures".

†Corresponding author. E-mail: xieyanwu@stanford.edu

© 2013 Chinese Physical Society and IOP Publishing Ltd

strated in this quasi-two-dimensional electron gas (q2DEG). Many of these properties can be largely attributed to the fact that the q2DEG is confined in the STO layer close to the interface. It is well known that bulk STO can host highly-mobile electrons[13] and can be doped into a superconductor.[14] However, the physical properties of the q2DEG are more than the simple extension of its bulk analogy. For example, the ferromagnetism is unexpected since both STO and LAO are non-magnetism materials; the coexistence of superconductivity and ferromagnetism is rare since they should typically repel each other in nature. This behavior is thus considered as emergent phenomena occurring at the interface. All these properties make the q2DEG rather exotic, showing significant importance for both the fundamental understanding of artificial materials and the potential applications in future oxide devices. Needless to say, all the properties of the q2DEG rely on the details of its synthesis, especially the carrier density and mobility. Therefore, it is crucial to find effective and flexible ways to tune the q2DEG.

In this paper, we will briefly review the experimental methods that have been used to tune the q2DEG and their recent progress. In Section 2, we give a few general considerations of the q2DEG based on electrostatics. In Section 3, we review the work in tuning the q2DEG by controlling the growth conditions, including the substrate, growth temperature, oxygen pressure, post annealing, LAO thickness, LAO stoichiometry, and the capping layer. In Section 4, we review the work in tuning the q2DEG by electrostatic field gating through the STO substrate or the LAO film. In Section 5, we review the work in tuning the q2DEG by scanning the LAO surface using a biased conductive atomic force microscopy probe. In Section 6, we review the work in tuning the q2DEG by surface adsorbates. Finally, we give concluding remarks in Section 7.

2. A few general considerations

Thus far, oxygen vacancies in STO,[15] atomic interdiffusion at the interface,[16] and the electronic reconstruction (as described in Section 1)[2] have been suggested to be the origin of the q2DEG. Whereas a number of features[17–19] support the notion that the electronic reconstruction must play a role as an intrinsic mechanism; in practice other mechanisms, such as oxygen vacancies,[15] also play a significant role in the properties of the q2DEG. The underlying consideration is the total system response to the electrochemical potential given the specific growth conditions.[20] In the following, without distinguishing the detailed mechanisms, we discuss a few general considerations of the system based on electrostatics.

Firstly, the fact that the q2DEG is confined in the STO layer close to the interface suggests that in that layer, there exists a potential well for electrons. This potential well has been observed in a few spectroscopic measurements.[21,22] Secondly, the LAO/STO structure as a whole must be charge-neutral in the absence of an external field.[23,24] It seems that there are only three conditions that fully meet the above two requirements. The first condition, as shown in Fig. 2(a), is that for a bulk stoichiometric surface, there are electrons transferring from the LAO side to the STO side, no matter what the real source of electrons is (e.g. defects in the bulk LAO film, the surface states of LAO, the valence band of the surface LAO or surface adsorbates). The second condition, similar to the first condition, is that there exist interfacial states which dope electrons in the STO. The third condition, as sketched in Fig. 2(b), is that there is a polarized STO layer which produces a potential well for electrons. In parallel, as sketched in Fig. 2(c), electrons trapped by oxygen vacancies in the bulk STO can flow to the potential well, leaving positive charges behind. This process in turn reduces the potential well, preventing the electrons from further transferring. Therefore, the q2DEG is in a delicate balance between two different processes: the process to transfer electrons and build up the potential well and the process to accumulate electrons but reduce the potential well. On the one hand, it is difficult to accurately control the q2DEG since it is sensitive to so

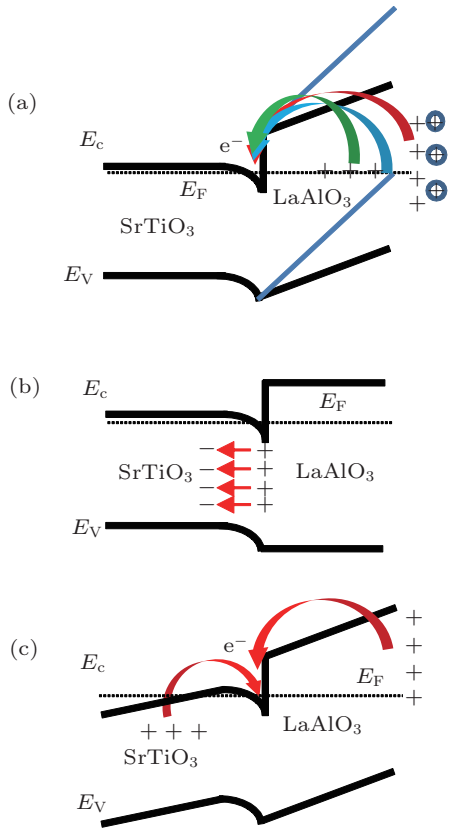


Fig. 2. Schematic illustrations of electron transfer and the interfacial potential well in LAO/STO. (a) Electrons move from the LAO to the STO. Independent of the electron source, a potential well for electrons is formed in the STO layer close to the interface. (b) Without the transfer of electrons from the surface (such as the case for surface reconstructions of LAO), a potential well can also be formed by the polarization of the STO layer. (c) Oxygen vacancies in the bulk STO transfer electrons to the interfacial potential well, leaving a positive charge behind. This process causes an electrical field to lower the potential well.

many factors. On the other hand, this sensitivity provides us with a variety of ways to tune the q2DEG.

3. Tuning the q2DEG by growth

The physical properties of the q2DEG are determined in the first place by the details of growth. Pulsed laser deposition has been a most widely used technique to grow LAO/STO samples, while molecular beam epitaxy[25,26] and sputtering[27] have also been used to grow the LAO/STO samples. Here we will restrict our discussion on the samples grown by pulsed laser deposition.

3.1. Substrate

The STO substrate is the most important parameter in determining the properties of the q2DEG since it hosts the q2DEG and is the starting block for stacking atomic layers of LAO. Methods to prepare high-quality TiO_2-terminated STO substrates have been well developed;[28] currently, these substrates are commercially available. As far as tuning the substrate is concerned, there are a few reports on changing surface termination,[1,2] lattice constant,[29] crystalline orientation[30,31] or doping[32] of STO. It was found that there is no q2DEG for LAO/STO samples grown on SrO-terminated STO.[1] By depositing STO films on different substrates, Bark *et al.*[29] tailored the lattice constant of STO by epitaxial stain. They studied the q2DEG formed by depositing LAO on these strained STO films and found that it is destroyed in tensile-strained STO but survives in compressively strained STO, with a reduced carrier density. In addition to the normal LAO/STO samples grown on (100) STO, the presence of q2DEG in samples grown on (110) and (111) STO have been recently reported.[30,31]

3.2. Growth temperature

A proper temperature is needed for growing the high-quality LAO films on STO. Previously, epitaxial LAO films have been grown on STO in a wide temperature range, from as low as 550 °C to higher than 850 °C, although the most typical growth temperature is around 800 °C. It was first demonstrated by Caviglia *et al.*[33] that samples of lower sheet carrier density, $n_{\rm sheet}$, and higher mobility, μ, can be obtained by simply reducing the growth temperature to $\sim$ 650 °C. The underlying mechanism is not yet clear. A possible aspect is that the lower growth temperature reduces interfacial diffusion, thus reducing the impurity scattering of the q2DEG. For comparison, in Fig. 3, we present the transport properties of two typical samples grown at 800 °C and 650 °C, respectively, with the same growth conditions except for the temperature. Both samples show metallic behaviors at temperatures down to 2 K. As expected, the sample grown at 650 °C has a lower $n_{\rm sheet}$ and higher μ.

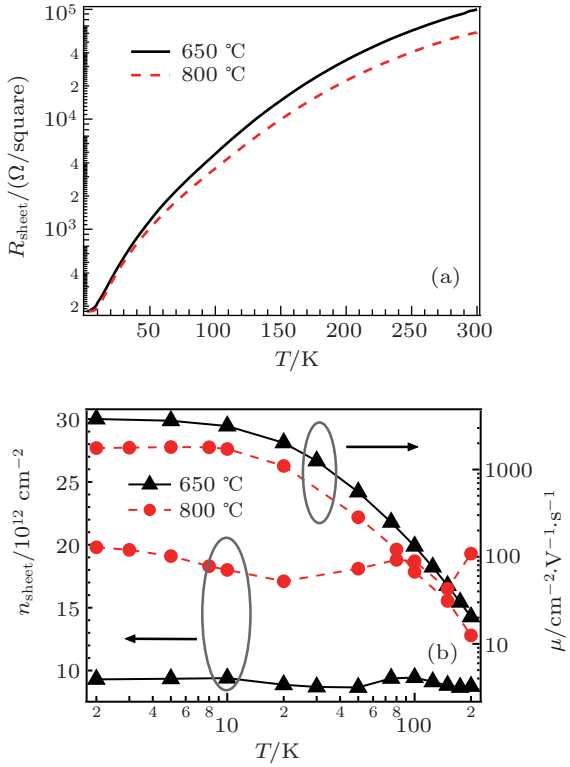


Fig. 3. Temperature dependences of (a) sheet resistance, $R_{\rm sheet}$ and (b) carrier density, $n_{\rm sheet}$, and mobility, μ, of typical samples grown at 800 °C and 650 °C. The LAO thickness values of the two samples are both 10 uc. The growth conditions are the same except for the growth temperature.

3.3. Oxygen pressure

The oxygen pressure during growth affects the oxygen content values in both the LAO film and the STO substrate and modifies the shape and species of the plume ejected from the LAO target. Therefore, it has an important influence on the properties of the q2DEG and thus can be used as a parameter for tuning. Figure 4 shows the temperature dependences of sheet resistance, $R_{\rm sheet}$, of samples grown under different oxygen pressures.[1,7] The low-temperature electrical transport evolves from metallic to semiconducting behavior with the increase of oxygen pressure. The values of $R_{\rm sheet}$ differ from each other by more than 6 orders of magnitude when the oxygen pressure increases from 1.0 $\times 10^{-4}$ Pa to 1.0×10^{-1} Pa. It has been recognized that the samples grown at a low oxygen pressure include a large number of oxygen vacancies. However, simply reducing the oxygen vacancies by increasing the oxygen pressure during growth is not ideal, for the mobility of the q2DEG is severely reduced. Instead, the most widely used method to prepare samples with minimized oxygen vacancies is to first grow the LAO film in a relatively low oxygen pressure range from 1.0×10^{-3} Pa to 1.0×10^{-2} Pa, followed by an *in situ* post annealing to refill oxygen at an oxygen pressure of more than 2.0×10^{4} Pa.[34]

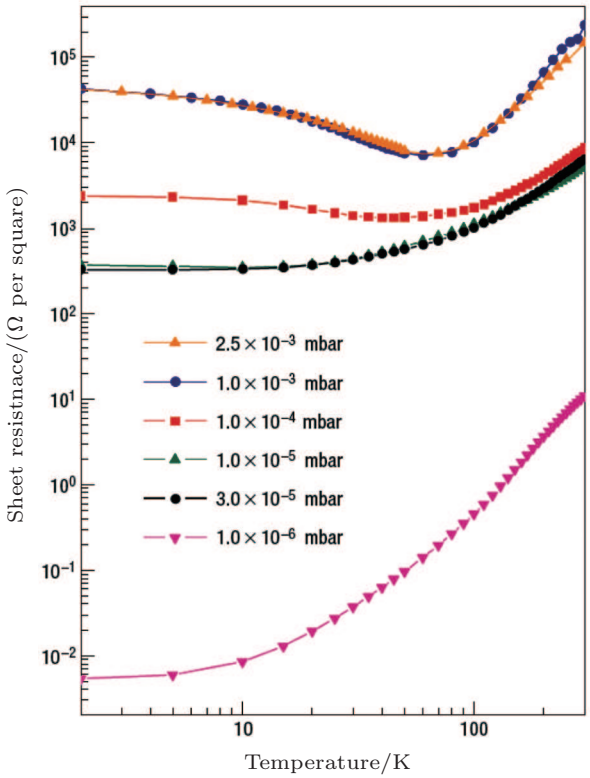


Fig. 4. Temperature dependences of sheet resistance of LAO/STO samples grown at various oxygen pressures. The figure is reproduced from Ref. [7]. The unit 1 bar = 10^5 Pa.

3.4. Post-annealing

The main purpose of post-annealing (in different environments) is to control the oxygen content values in the samples without affecting the growth kinetics. As discussed in Subsection 3.3, post-annealing often accompanies a typical growth, to insure that the samples can reach the stoichiometric oxygen content values. It should be mentioned that the STO substrate itself (without depositing LAO) is still transparent and highly insulating after experiencing the same temperature and oxygen pressure for the growth of the LAO film. Therefore, the density of oxygen vacancies in the STO substrate is at a level lower than that in the presence of detectable bulk conduction. However, the effect of oxygen vacancies is amplified by the interfacial potential well, which accumulates electrons trapped by oxygen vacancies to the interface. Therefore, it is not surprising that the properties of the q2DEG are very sensitive to the conditions of post-annealing. In addition, if samples have been exposed to an ambient environment before post-annealing, its effect will become much more complicated since the variation of surface adsorbates is potentially involved. This issue will be discussed in Section 6.

3.5. LAO thickness

The LAO thickness has been known to be a crucial tuning parameter of the q2DEG. A key feature of the LAO/STO heterostructure is that there is a critical thickness of LAO of around 3 uc–4 uc.[34] Below this thickness, the sample is insulating; above it, the sample is conducting. The existence of this critical thickness has been suggested to support the electronic reconstruction model. However, under the assumption of an unreconstructed LAO surface, $n_{\rm sheet}$ will continue to increase with the increase of LAO thickness above this critical thickness.[35] As shown in Fig. 5, experimentally there are often no clear trends between $n_{\rm sheet}$ and the LAO thickness for beyond the critical thickness.[36] This indicates that the LAO surface reconstruction must play a role with thickness varying. As far as the conductivity is concerned, the highest quality

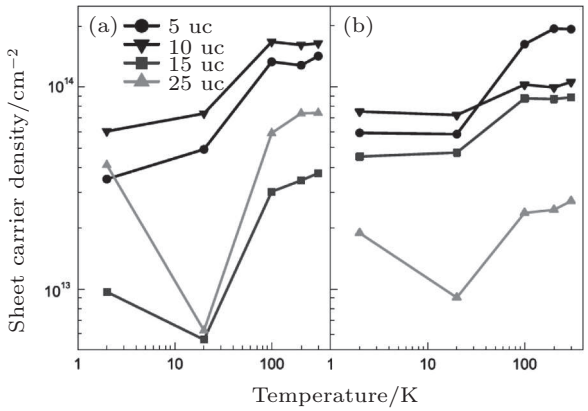


Fig. 5. Temperature dependences of the sheet carrier density of LAO/STO samples for various LAO thickness values at oxygen pressures of (a) 1.33 mPa and (b) 13.3 mPa during growth. The figure is reproduced from Ref. [36].

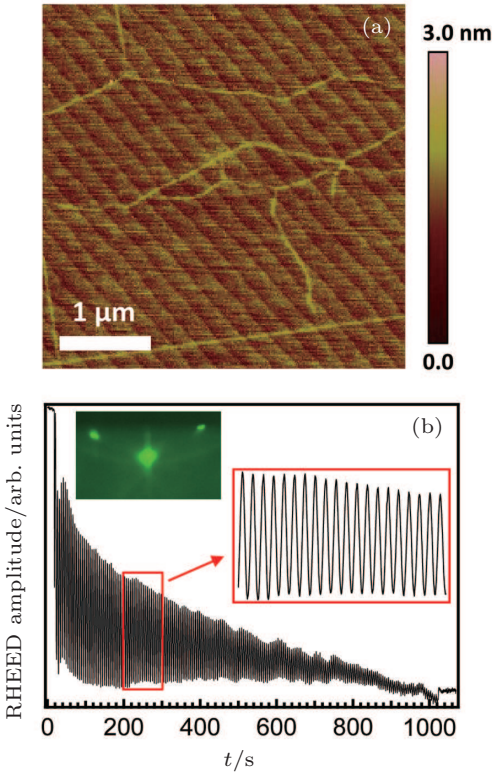


Fig. 6. (a) AFM surface morphology of a typical LAO(25 uc)/STO sample grown at 800 °C. (b) Oscillations of the RHEED amplitude of an LAO(200 uc)/STO sample grown at 650 °C.

beyond samples are generally prepared with an LAO thickness below 15 uc. Above this value, many cracks often appear due to the release of strain (the lattice mismatch between STO and LAO is $\sim 3\%$) (Fig. 6(a)). The interfacial conductivity often becomes much smaller when LAO is very thick, although the relevant reports can be rarely found. Figures 6(b) show the reflection high-energy electron diffraction (RHEED) oscillations of a sample with an LAO thickness of 200 uc, grown at 650 °C. The clear RHEED oscillations suggest that the LAO film was grown well in a two-dimensional growth mode. However, the sample is insulating with a resistance $>$ GΩ at room temperature. This phenomenon is not yet well understood and suggests the further evolution of the electronic structure even for very thick samples.

3.6. (Non) stoichiometry of the LAO film

It is a natural expectation that the (non)stoichiomety of the LAO film has a large influence on the properties of the q2DEG since it is directly related to the built-in potential in LAO, the driving force of the q2DEG. Reinle-Schmitt *et al.*[19] grew $(LAO)_{1-x}(STO)_x$ (STO-diluted LAO) films on TiO_2-terminated STO substrates and found that the critical thickness for the formation of the q2DEG increases with the increase of x, demonstrating the correlation between the q2DEG and the built-in potential in LAO. In a few recent studies[26,37,38] the stoichiometry of LAO, i.e., the atomic ratio of La/Al was intentionally modified to tune the properties of the q2DEG. As shown in Fig. 7, Sato *et al.*[37] tuned the La/Al ratio of the LAO film by using different laser fluences and found that both the lattice constant of the film and the conductivity have a systematic change with the La/Al ratio.

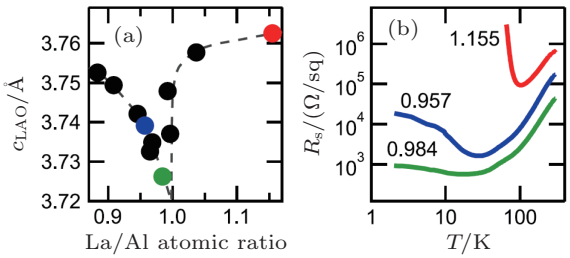


Fig. 7. (a) Out-of-plane lattice constant of the epitaxial LAO film as a function of the cation ratio. (b) Temperature dependence of the sheet resistance of LAO/STO samples of different cation ratios. The figure is reproduced from Ref. [37].

3.7. Capping layer

The properties of the q2DEG can be effectively tuned by choosing proper capping layers. From first-principles calculations and experiments, Pentcheva *et al.*[39] showed that even a single monolayer of a nonpolar material has a crucial influence on the electronic reconstruction at the interface. They found that while LAO(2uc)/STO is insulating (below the critical thickness), it becomes conducting after being capped with an additional 1-uc STO. The effect of various metal capping layers on the q2DEG has also been calculated.[40] Experimentally, in addition to STO, $SrCuO_2$,[41] $YBa_2Cu_3O_7$[42] and $La_{1-x}Sr_xMnO_3$[43] have been used as capping layers to tune the q2DEG. Huijben *et al.*[41] showed that the mobility of the q2DEG can be enhanced to more than 5500 $cm^2 \cdot V^{-1} \cdot s^{-1}$ by capping the LAO/STO structures with 1 uc–3 uc of $SrCuO_2$ and 2-uc STO. The improvement on mobility has been ascribed to the reduction of the density of defect states by the remote $SrCuO_2$ layer. Ferroelectric materials, such as $Pb(Zr_{0.2}Ti_{0.8})O_3$, have also been used to cap the LAO/STO.[44,45] The polarization of ferroelectric material can be controlled reversibly by an external electrical bias, so the nonvolatile tuning of the q2DEG has been achieved.

4. Tuning the q2DEG by electrostatic field gating

Electrostatic field effect is an ideal tool to modulate the q2DEG since it allows the controllable and reversible variation of n_{sheet} without changing the microstructure and chemical composition of the system. The insulating natures of both STO and LAO allow two assessable approaches to the electrostatic gating: back gating through the STO substrate and top gating through the LAO film.

4.1. Back gating through the STO substrate

Back gating is the most widely used approach to tune the q2DEG beyond growth. As sketched in Fig. 8(a), the device can be arranged by simply applying an electrical bias between the LAO/STO interface and a metallic electrode attached to the backside of the STO substrate. Since STO has an extremely large low-temperature dielectric constant ($\sim 2 \times 10^4$ at $T = 2$ K),[46] it is possible to achieve a large tuning of n_{sheet} with a moderate bias. Using this method, Thiel *et al.*[34] have pushed the insulating LAO(3 uc)/STO samples (below the critical thickness) to become metallic; Caviglia *et al.*[6] have continuously tuned the transport behavior of the q2DEG from an insulating to a superconducting state (Figs. 8(b) and 8(c)) and revealed a dome of superconductivity with the electrical bias. In addition to the modulation of n_{sheet}, Bell *et al.*[47] demonstrated that the mobility of the q2DEG has an even larger change than n_{sheet}. As shown in Fig. 9, while n_{sheet} decreases by $\sim 40\%$ when the gate voltage decreases from $+100$ V to -50 V, the mobility decreases by more than one order of magnitude. It was proposed that the profile of the interfacial potential well is changed by the gating through STO, which in turn changes the spatial distribution of the q2DEG.[47] A negative (positive) bias pushes the q2DEG close to (away from) the interface. Since the density of scattering sites is high in the region close to the interface, the mobility of the q2DEG is low when it is close to the interface.[15,47] Currently, more

and more attention has been paid to quantum transport effects in the q2DEG; thus lower $n_{\rm sheet}$ and high mobility are highly desired. In this sense, back gating itself is not always ideal for this purpose.

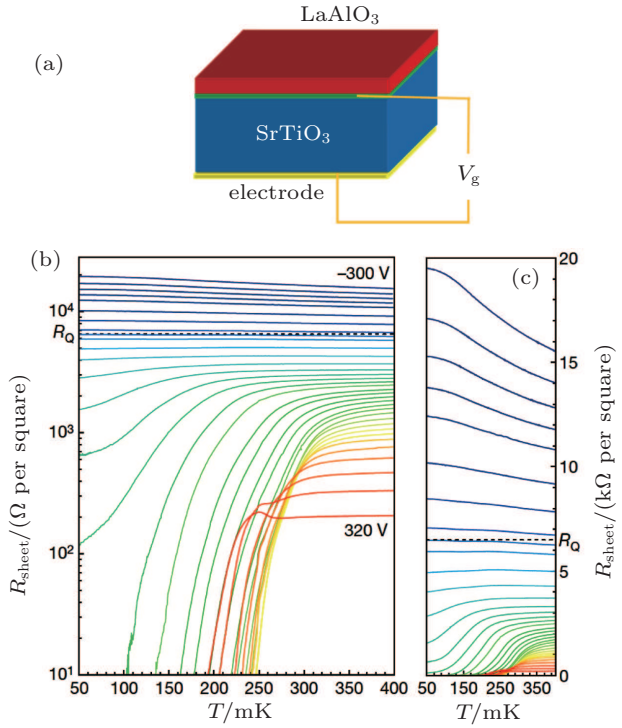


Fig. 8. (a) Schematic illustration of back gating through STO. (b) Plots of measured sheet resistance versus temperature on a semi-logarithmic scale, for gate voltages varying from −300 V to 320 V. The dashed line indicates the quantum of pair resistance. (c) The same data plotted on a linear resistance scale. Panels (b) and (c) are reproduced from Ref. [6].

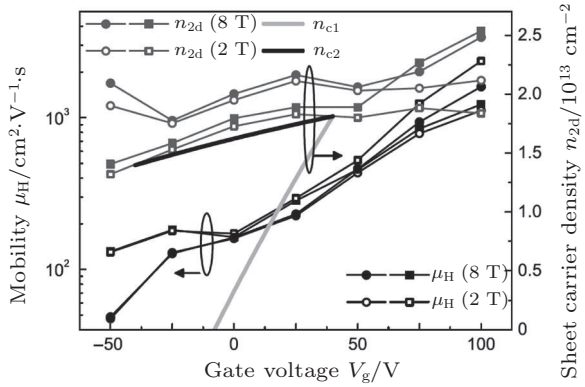


Fig. 9. Plots of sheet carrier density and mobility versus gate voltage, at $T = 0.1$ K (squares) and $T = 2$ K (circles). Closed and open symbols refer to high field (8 T) and low field (2 T) values of the Hall coefficient, respectively. Lines are guides to the eye. The figure is reproduced from Ref. [47].

4.2. Top gating through the LAO film

LAO has been regarded as a potential candidate as a high dielectric constant (~ 25) gate dielectric for the substitution of SiO_2 in semiconductor field effect transistors.[48,49] However, there are much fewer reports using top gating through the LAO film to tune the q2DEG than using the back gating. The main reason is that the typical $n_{\rm sheet}$ of the q2DEG is about one order of magnitude larger than that of traditional 2DEGs; thus a much larger electric field is needed to achieve the effective tuning. In addition, there are two more complications which make it difficult to use LAO as a gating dielectric in the LAO/STO structure. First, as discussed in Subsection 3.7, the gating electrode deposited on the LAO surface can significantly change the q2DEG as a capping layer. Second, the electric field is applied through the LAO film, which can significantly change the potential in the LAO and thus the electronic reconstruction. Förg *et al.*[42] reported on the first field-effect device through gating LAO (Fig. 10). By capping 40 nm of $YBa_2Cu_3O_7$ film (which also works as the top electrode) on the LAO/STO surface, they reduced $n_{\rm sheet}$ to the order of 10^{12} cm^{-2}. After that, they can tune the interfacial q2DEG effectively using gating through the LAO. Recently, by optimizing the growth condition and electrode materials, Hosoda *et al.*[50] demonstrated successful tuning of samples of much larger $n_{\rm sheet}$. Interestingly, in contrast to the use of back gating, they found that with top gating, the decrease of $n_{\rm sheet}$ is accompanied by the increase of mobility, providing a route to obtaining q2DEGs of low $n_{\rm sheet}$ and high mobility.

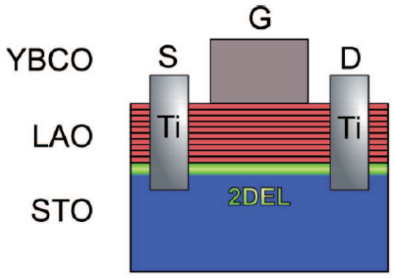


Fig. 10. Sketch of the cross section of a top gating field-effect device using LAO(9 uc)/STO. Let S, G and D stand for source, gate and drain, respectively. The figure is reproduced from Ref. [42].

5. Tuning the q2DEG by conductive atomic force microscopy (CAFM)

It was first demonstrated by Cen *et al.*[51,52] that a positively biased CAFM probe can create a conductive path from the insulating LAO/STO samples that are just below the critical thickness (Fig. 11). The induced conductive path can also be cut off by a negatively biased probe. The width of the conductive feature can be as narrow as a few nm, intriguing for future oxide nano electronics. In following work,[53] we demonstrated that the paths written by the CAFM probe can be directly detected by several electrical force microscopy techniques. As shown in Fig. 12, the paths written by positive and negative bias have reverse contrast. These observations suggest that the change of the interfacial conductivity can be attributed to surface charges injected from the biased CAFM probe, acting like a local top gate in some sense. We further found that the surface charges are stable in LAO/STO samples

thicker than the critical thickness and can be readily written over a relatively large area (Fig. 13).[54] These observations suggest the possibility of tuning the q2DEG by CAFM.

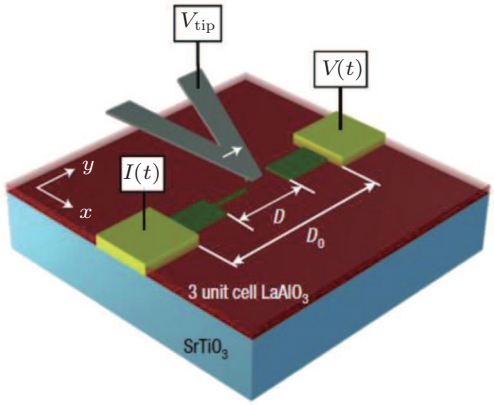


Fig. 11. Schematic diagram of writing a conducting wire on an insulating LAO(3 uc)/STO sample. A biased CAFM tip is scanned from one electrode towards a second one in contact mode and a metallic q2DEG is formed locally at the interface under the route of the tip. The figure is reproduced from Ref. [51].

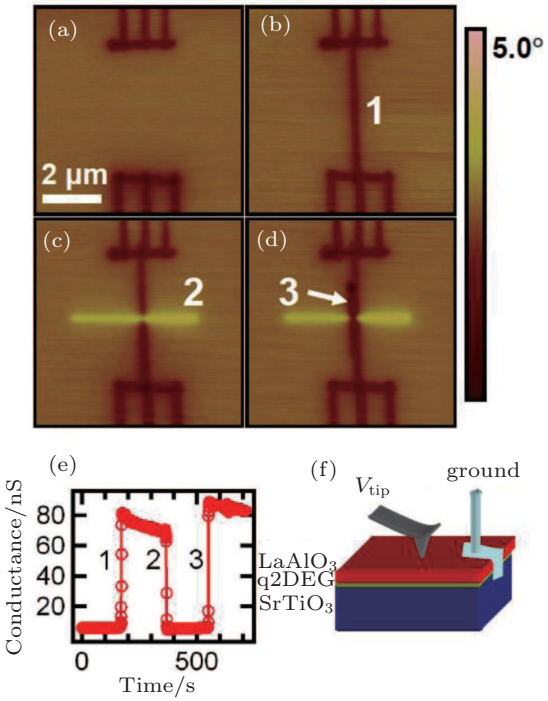


Fig. 12. Writing and erasing conductive paths for an LAO(3 uc)/STO sample. Electrical force microscopy phase images with $V_{read} = -2$ V. (a) Dark contrast shows the electrodes connected to the outer Al wiring, $V_{write} = +8$ V. (b) The written wire connects the electrodes, $V_{write} = +6$ V, corresponding to number 1 in panel (e). (c) The wire is cut (bright phase contrast) with $V_{write} = -3$ V, corresponding to number 2 in panel (e). (d) Electrodes reconnected with a vertical line using $V_{write} = +6$ V, corresponding to number 3 in panel (e). (e) Two point-conductance between the outer Al electrodes. (f) Schematic AFM writing. The figure is reproduced from Ref. [53].

We have employed CAFM to tune the q2DEG in typical samples.[54,55] As shown in the inset of Fig. 14(a), the sample has been patterned into a Hall bar and the entire active area was scanned. Figures 14(b) and 14(c) show that the positive charges increase n_{sheet} in the entire temperature range, accompanied by the decrease of mobility; in contrast, negative writing reduces n_{sheet}, accompanied by the increase of mobility. Since the mobility of the q2DEG shows a significant increase with the decrease of n_{sheet} in the CAFM tuning, it is promising to be used to prepare q2DEG for quantum transport.[55] By varying a few writing parameters, such as voltage, we can tune n_{sheet} over a large range, with a maximum tuning

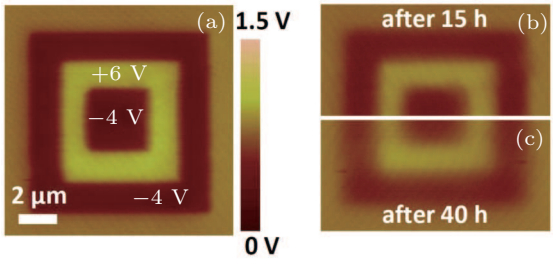


Fig. 13. (a) Surface-potential image of an electrostatic pattern written on an LAO(5 uc)/STO sample. The pattern was achieved by first writing a 9 μm×9 μm square with $V_{write} = -4$ V, then a 6×6 μm^2 square with $V_{write} = +6$ V on the top of the first square, and finally a 3 μm×3 μm square with $V_{write} = -4$ V in the center of the image. The surface-potential image of the same pattern is also shown after waiting for 15 h (b) and 40 h (c) in an ambient environment. The scale bar used in panel (a) is also for all of the images. The figure is reproduced from Ref. [54].

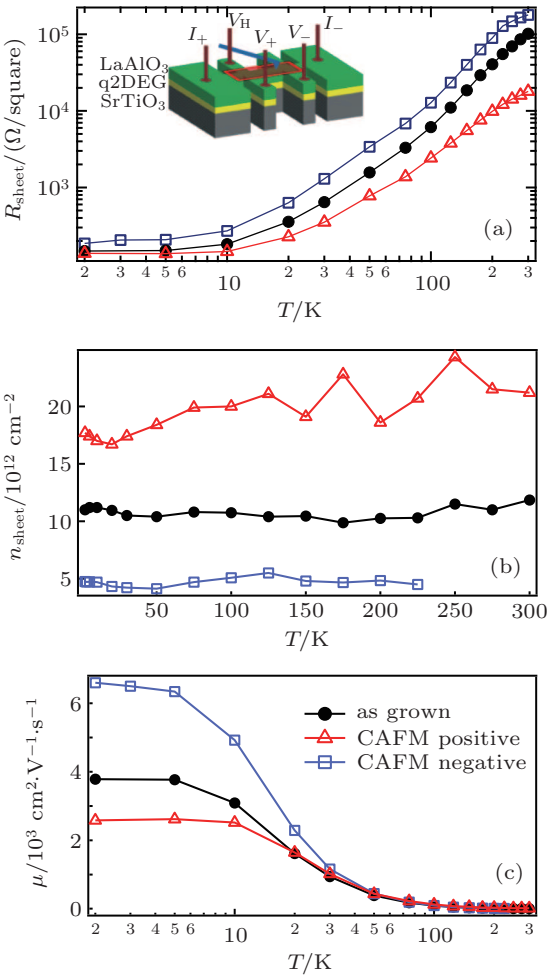


Fig. 14. Tuning the q2DEG by CAFM. Temperature dependences of (a) R_{sheet}, (b) n_{sheet}, and (c) mobility μ of a typical sample in the as-grown state (closed circles), after CAFM positive tuning (open triangles), and after CAFM negative tuning (open squares). Lines are guides for the eye. The sample was grown at 650 °C, with an LAO thickness of 9 uc and patterned into a 10-μm wide Hall bar. The figure is reproduced from Ref. [55].

ability comparable to that of the normal gating effect.[54] A major limitation of CAFM tuning is the decay of charges. As shown in Fig. 13, the surface charge may decay severely over 40 h. This problem can be partially resolved by storing the written samples in a vacuum.[52]

6. Tuning the q2DEG by surface adsorbates

It was found that the q2DEG can be dramatically changed by exposing samples to a variety of common laboratory solvents, such as acetone, ethanol, and water.[18] As shown in Fig. 15(a), $R_{\rm sheet}$ decreases significantly after exposure to water on the surface of the LAO. This phenomenon can be related to the adsorption of solvent molecules on the surface of the LAO. As shown in Fig. 15(b), this treatment can change an $n_{\rm sheet}$ from around 1×10^{13} cm^{-2} to more than 3×10^{13} cm^{-2}. Heating the solvent-treated samples at a moderate temperature can desorb the adsorbates and recover the original q2DEG. As shown in Fig. 16, the influence of the solvents on the q2DEG is controlled by the polarity of solvents. These observations provide a flexible way to tune the q2DEG by adsorption and desorption

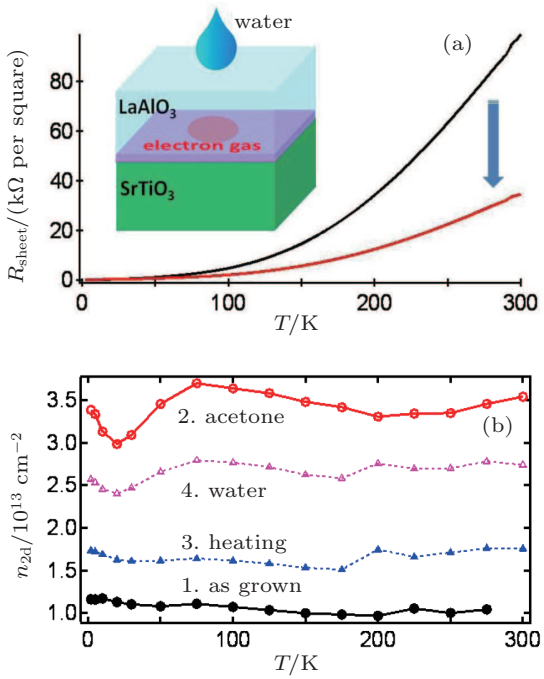


Fig. 15. (a) Temperature dependences of $R_{\rm sheet}$ before and after exposing an LAO(10 uc)/STO sample to a solvent. (b) Temperature dependences of the sheet carrier density, $n_{\rm 2d}$, for the sample in different states. The solid circles represent the data from the as-grown sample before experiencing any solvent. The empty circles represent the data from the sample after treating by acetone. The solid triangles represent the data from the sample after heating at $T = 390$ °C in an O_2 pressure of 1.33×10^{-2} Pa for 5 h. The empty triangles represent the data from the sample after treating by water. The treating and measurement sequence is marked with numbers in panel (b). The figure 15(b) is reproduced from Ref. [18].

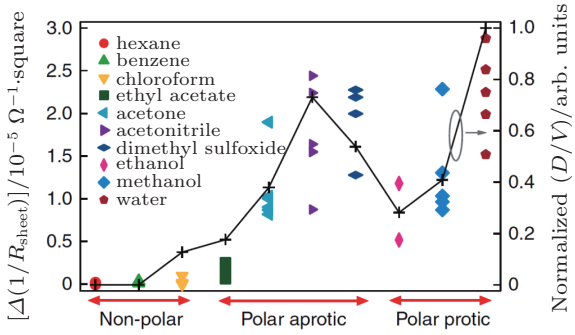


Fig. 16. Effect of adsorbates on the q2DEG for different solvents. The difference in $1/R_{\rm sheet}$ between after and before solvent treatment, $\Delta(1/R_{\rm sheet})$, reflects the change in $n_{\rm sheet}$ at room temperature. A clear increase in $\Delta(1/R_{\rm sheet})$ is observed after surface treatment using polar solvents, independent of their aprotic or protic characteristic. $\Delta(1/R_{\rm sheet})$ is reasonably scaled with the molecular dipole moment (D) of each solvent, divided by the corresponding molecular volume ($V_{\rm m}$) (crosses). The line is a guide to the eye. At least two samples were used for each solvent and all samples were LAO(10 uc)/STO and in the as-grown state before treatment. The figure is reproduced from Ref. [18].

of molecules with different polarities. It should be noted that all practical samples that have been used for transport measurements have been exposed to air. Therefore, the q2DEG in all of these cases has been modified by water adsorbates to some degree. These results further suggest that many of the different properties reported in the literature may be due to this unusual phenomenon and strongly affect comparisons between *in situ* and *ex situ* studies.

7. Concluding remarks

In the preceding sections, we have shown that the q2DEG can be tuned by a variety of methods, from growth to beyond growth. This list of methods is not complete in any sense. For example, as is well known, the LAO/STO is sensitive to light,[51] which can work as an additional degree of freedom in tuning the q2DEG. It is also promising to tune the q2DEG using the ionic liquid gating technique,[3,56] which has emerged as a powerful way to achieve large tuning of $n_{\rm sheet}$. Despite all of these available methods, it is still a great challenge to control the q2DEG accurately. Often one needs to combine several different methods to achieve a q2DEG of desired properties. It is interesting to note that the tuning of most methods follows a general trend that mobility increases with the decrease of $n_{\rm sheet}$ (Fig. 17), indicating their intrinsic correlation. We expect that the combination and optimization of these different methods can enable us to enter into a region where the quantum transport of the q2DEG can be studied in detail. Finally, these methods developed for tuning the q2DEG in LAO/STO may also have general applications for tuning electrons in other oxide heterostructures.

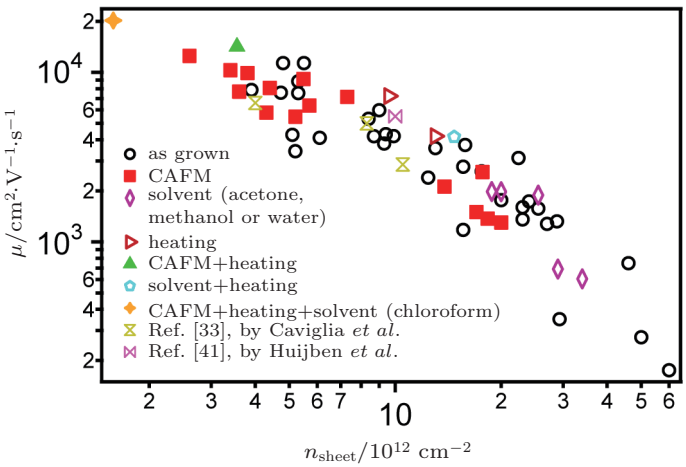


Fig. 17. Plots of mobility μ versus $n_{\rm sheet}$ for samples tuned by various methods. The thickness values of LAO films vary from 5 uc to 10 uc. The growth temperature varies from 600 °C to 800 °C. All samples are patterned into Hall bars with widths varying from 5 μm to 10 μm. For samples treated by more than one method, the sequence of the treatments is indicated in the labels. For example, "CAFM + heating" means first performing CAFM treatment and then heating treatment. All the data were measured at 2 K or below. The figure is reproduced from Ref. [55].

References

[1] Ohtomo A and Hwang H Y 2004 *Nature* **427** 423
[2] Nakagawa N, Hwang H Y and Muller D A 2006 *Nat. Mater.* **5** 204
[3] Hwang H Y, Iwasa Y, Kawasaki M, Keimer B, Nagaosa N and Tokura Y 2012 *Nat. Mater.* **11** 103
[4] Mannhart J, Blank D H A, Hwang H Y, Millis A J and Triscone J M 2008 *MRS Bull.* **33** 2027
[5] Reyren N, Thiel S, Caviglia A D, Fitting Kourkoutis L, Hammerl G, Richter C, Schneider C W, Kopp T, Rüetschi A S, Jaccard D, Gabay M, Muller D A, Triscone J M and Mannhart J 2007 *Science* **317** 1196
[6] Caviglia A D, Gariglio S, Reyren N, Jaccard D, Schneider T, Gabay M, Thiel S, Hammerl G, Mannhart J and Triscone J M 2008 *Nature* **456** 624
[7] Brinkman A, Huijben M, Van Zalk M, Huijben J, Zeitler U, Maan J C, Van Der Wiel W G, Rijnders G, Blank D H A and Hilgenkamp H 2007 *Nat. Mater.* **6** 493
[8] Ariando, Wang X, Baskaran G, Liu Z Q, Huijben J, Yi J B, Annadi A, Roy Barman A, Rusydi A, Dhar S, Feng Y P, Ding J, Hilgenkamp H and Venkatesan T 2011 *Nat. Commun.* **2** 188
[9] Lee J S, Xie Y W, Sato H K, Bell C, Hikita Y, Hwang H Y and Kao C C 2013 *Nat. Mater.* **12** 703
[10] Bert J A, Kalisky B, Bell C, Kim M, Hikita Y, Hwang H Y and Moler K A 2011 *Nat. Phys.* **7** 767
[11] Li L, Richter C, Mannhart J and Ashoori R C 2011 *Nat. Phys.* **7** 762
[12] Dikin D A, Mehta M, Bark C W, Folkman C M, Eom C B and Chandrasekhar V 2011 *Phys. Rev. Lett.* **107** 056802
[13] Tufte O N and Chapman P W 1967 *Phys. Rev.* **155** 796
[14] Schooley J F, Hosler W R and Cohen M L 1964 *Phys. Rev. Lett.* **12** 474
[15] Siemons W, Koster G, Yamamoto H, Harrison W A, Lucovsky G, Geballe T H, Blank D H A and Beasley M R 2007 *Phys. Rev. Lett.* **98** 196802
[16] Willmott P R, Pauli S A, Herger R, Schleputz C M, Martoccia D, Patterson B D, Delley B, Clarke R, Kumah D, Cionca C and Yacoby Y 2007 *Phys. Rev. Lett.* **99** 155502
[17] Schlom D G and Mannhart J 2011 *Nat. Mater.* **10** 168
[18] Xie Y W, Hikita Y, Bell C and Hwang H Y 2011 *Nat. Commun.* **2** 494
[19] Reinle-Schmitt M L, Cancellieri C, Li D, Fontaine D, Medarde M, Pomjakushina E, Schneider C W, Gariglio S, Ghosez Ph, Triscone J M and Willmott P R 2012 *Nat. Commun.* **3** 932
[20] Higuchi T and Hwang H Y 2012 in *Multifunctional Oxide Heterostructures*, ed. Tsymbal E, Dagotto E R A, Eom C B and Ramesh R (Oxford: Oxford University Press) Chap. 7
[21] Yoshimatsu K, Yasuhara R, Kumigashira H and Oshima M 2008 *Phys. Rev. Lett.* **101** 026802
[22] Huang B C, Chiu Y P, Huang P C, Wang W C, Tra V T, Yang J C, He Q, Lin J Y, Chang C S and Chu Y H 2012 *Phys. Rev. Lett.* **109** 246807
[23] Bristowe N C, Littlewood P B and Artacho E 2011 *Phys. Rev. B* **83** 205405
[24] Ibbetson J P, Fini P T, Ness K D, DenBaars S P, Speck J S and Mishra U 2000 *Appl. Phys. Lett.* **77** 250
[25] Segal Y, Ngai J H, Reiner J W, Walker F J and Ahn C H 2009 *Phys. Rev. B* **80** 241107
[26] Warusawithana M P, Richter C, Mundy J A, Roy P, Ludwig J, Paetel S, Heeg T, Pawlicki A A, Kourkoutis L F, Zheng M, Lee M, Mulcahy B, Zander W, Zhu Y, Schubert J, Eckstein J N, Muller D A, Hellberg C S, Mannhart J and Schlom D G 2013 *Nat. Commun.* **4** 235
[27] Dildar I M, Boltje D B, Hesselberth M H S, Aarts J, Xu Q, Zandbergen H W and Harkema S 2013 *Appl. Phys. Lett.* **102** 121601
[28] Kawasaki M, Takahashi K, Maeda T, Tsuchiya R, Shinohara M, Ishiyama O, Yonezawa T, Yoshimoto M and Koinuma H 1994 *Science* **266** 1540
[29] Bark C W, Felker D A, Wang Y, Zhang Y, Jang H W, Folkman C M, Park J W, Baek S H, Zhou H, Fong D D, Pan X Q, Tsymbal E Y, Rzchowski M S and Eom C B 2011 *Proc. Natl. Acad. Sci.* **108** 4720
[30] Herranz G, Sanchez F, Dix N, Scigaj M and Fontcuberta J 2012 *Sci. Rep.* **2** 758
[31] Annadi A, Zhang Q, Wang X R, Tuzla N, Gopinadhan K, Lü W M, Barman A R, Liu Z Q, Srivastava A, Saha S, Zhao Y L, Zeng S W, Dhar S, Olsson E, Gu B, Yunoki S, Maekawa S, Hilgenkamp H, Venkatesan T and Ariando 2013 *Nat. Commun.* **4** 1838
[32] Fix T, Schoofs F, MacManus-Driscoll J L and M G Blamire 2010 *Appl. Phys. Lett.* **97** 072110
[33] Caviglia A D, Gariglio S, Cancellieri C, Sacépé B, Fête A, Reyren N, Gabay M, Morpurgo A F and Triscone J M 2010 *Phys. Rev. Lett.* **105** 236802
[34] Thiel S, Hammerl G, Schmehl A, Schneider C W and Mannhart J 2006 *Science* **313** 1942
[35] Schwingenschlögl U and Schuster C 2008 *Europhys. Lett.* **81** 17007
[36] Bell C, Harashima S, Hikita Y and Hwang H Y 2009 *Appl. Phys. Lett.* **94** 222111
[37] Sato H K, Bell C, Hikita Y and Hwang H Y 2013 *Appl. Phys. Lett.* **102** 251602
[38] Breckenfeld E, Bronn N, Karthik J, Damodaran A R, Lee S, Mason N and Martin L W 2013 *Phys. Rev. Lett.* **110** 196804
[39] Pentcheva R, Huijben M, Otte K, Pickett W E, Kleibeuker J E, Huijben J, Boschker H, Kockmann D, Siemons W, Koster G, Zandvliet H J W, Rijnders G, Blank D H A, Hilgenkamp H and Brinkman A 2010 *Phys. Rev. Lett.* **104** 166804
[40] Arras R, Ruiz V G, Pickett W E and Pentcheva R 2012 *Phys. Rev. B* **85** 125404
[41] Huijben M, Koster G, Molegraaf H J A, Kruize M K, Wenderich S, Kleibeuker J E, McCollam A, Guduru V K, Brinkman A, Hilgenkamp H, Zeitler U, Maan J C, Blank D H A and Rijnders G 2010 preprint at http://arxiv.org/abs/1008.1896
[42] Förg B, Richter C and Mannhart J 2012 *Appl. Phys. Lett.* **100** 053506
[43] Shi Y J, Wang S, Zhou Y, Ding H F and Wu D *Appl. Phys. Lett.* **102** 071605
[44] Tra V T, Chen J W, Huang P C, Huang B C, Cao Y, Yeh C H, Liu H J, Eliseev E A, Morozovska A N, Lin J Y, Chen Y C, Chu M W, Chiu P W, Chiu Y P, Chen L Q, Wu C L and Chu Y H 2013 *Adv. Mater.* **25** 3357
[45] Kim S I, Kim D H, Kim Y J, Moon S Y, Kang M G, Choi J K, Jang H W, Kim S K, Choi J W, Yoon S J, Chang H J, Kang C Y, Lee S, Hong S H, Kim J S and Baek S H 2013 *Adv. Mater.* **25** 4612
[46] Sakudo T and Unoki H 1971 *Phys. Rev. Lett.* **26** 851
[47] Bell C, Harashima S, Kozuka Y, Kim M, Kim B G, Hikita Y and Hwang H Y 2009 *Phys. Rev. Lett.* **103** 226802
[48] Edge L F, Schlom D G, Chambers S A, Cicerrella E, Freeouf J L, Holländer B and Schubert J 2004 *Appl. Phys. Lett.* **84** 726
[49] Först C J, Schwarz K and Blöchl P E 2005 *Phys. Rev. Lett.* **95** 137602
[50] Hosoda M, Hikita Y, Hwang H Y and Bell C 2013 *Appl. Phys. Lett.* **103** 103507
[51] Cen C, Thiel S, Hammerl G, Schneider C W, Andersen K E, Hellberg C S, Mannhart J and Levy J 2008 *Nat. Mater.* **7** 298
[52] Cen C, Thiel S, Mannhart J and Levy J 2009 *Science* **323** 1026
[53] Xie Y W, Bell C, Yajima T, Hikita Y and Hwang H Y 2010 *Nano Lett.* **10** 2588
[54] Xie Y W, Bell C, Hikita Y and Hwang H Y 2011 *Adv. Mater.* **23** 1744
[55] Xie Y W, Bell C, Hikita Y, Harashima S and Hwang H Y 2013 *Adv. Mater.* **25** 4735
[56] Yuan H T, Shimotani H, Tsukazaki A, Ohtomo A, Kawasaki M and Iwasa Y 2009 *Adv. Funct. Mater.* **19** 1046